

Supporting Information

A Li⁺ Conductive Metal Organic Framework Electrolyte Boosts the High-Temperature Performance of Dendrite-Free Lithium Batteries

Nan Chen ^{a,†}, Yuejiao Li ^{a,†}, Yujuan Dai ^a, Wenjie Qu ^a, Yi Xing ^a, Yusheng Ye ^a, Ziyue Wen ^a, Cui Guo ^a, Feng Wu ^{a,b}, Renjie Chen ^{*a,b}

^a School of Materials Science & Engineering, Beijing Key Laboratory of Environmental Science and Engineering, Beijing Institute of Technology, Beijing 100081, China.

^b Collaborative Innovation Center of Electric Vehicles in Beijing, Beijing 100081, China.

[†]These authors contributed equally to this work and should be considered co-first authors.

* Corresponding Author, E-mail: chenrj@bit.edu.cn

Experimental Section

Materials: Reagents included Co(NO₃)₂·6H₂O (99.99%, J&K Chemicals, China), anhydrous methanol (99.9%, Aladdin, China), 2-methyl imidazole (99%, J&K Chemicals, China), N-propyl-N-methylpyrrolidinium bis(trifluoromethylsulfonyl) imide ([Py13][TFSI], >99%, Shanghai Cheng Jie, China), and lithium bis(trifluoromethylsulfonyl) imide (LiTFSI, >99%, 3M, USA, dried at 80 °C under vacuum for 48 h and subsequently placed in a glove box). Other materials were purchased and used without further purification.

Synthesis: ZIF-67 was prepared by a melt-stirring method. Co(NO₃)₂·6H₂O (8.22 g) and 2-methyl imidazole (18.5 g) were dissolved separately in 400 mL quantities of anhydrous methanol, after which the two solutions were mixed using a peristaltic pump at a flow rate of 100 mL·min⁻¹. During this process, the color of the Co(NO₃)₂·6H₂O solution changed from red to purple. The solution was allowed to sit overnight at room temperature (25 °C) and a purple solid precipitate was obtained. After centrifugation at 5 °C and drying at 60 °C for 24 h, the ZIF-67 was collected. The ionic liquid electrolyte (ILE) was obtained by mixing [Py13][TFSI] with LiTFSI in a glove box. The ILE@MOF electrolytes were prepared by high energy ball milling. In this process, the desired amounts of ZIF-67 and ILE were combined at a 2:3 mass ratio in a zirconia vial and subjected to high energy ball milling for 1 h in an Ar-filled dry box at a rate of 300 r·min⁻¹. The resulting ILE@MOF was rolled into a 50-μm-thick film and cut into free-standing pieces to allow for electrochemical measurements.

Characterization and instruments: The morphologies and microstructural features of the materials were examined using scanning electron microscopy (SEM; FEI Quanta 600). Surface areas were determined by nitrogen gas absorption in conjunction with the Brunauer–Emmett–Teller (BET) method, using an Autosorb-iQ2-MP analyzer. X-Ray powder diffraction (XRD) was performed over the 2θ range from 5° to 90° at a scanning rate of 2°·min⁻¹ with an X-ray diffractometer (Rigaku, Japanese), employing Cu-Kα radiation at 40 kV and 40 mA. Thermogravimetric analysis (TGA) was carried out under an Ar flow from ambient to 700 °C at a heating rate of 10 °C·min⁻¹ using a Netzsch TG209F1 analyzer. Fourier Transform

infrared spectroscopy (FTIR) was performed with a Nicolet 6700 FTIR spectrometer over the wavelength range of 400–4000 cm^{-1} and at a resolution of 4 cm^{-1} . Flammability tests of the ILE@MOF were carried out using an electronic Bunsen burner. In these trials, the ILE@MOF electrolyte was placed in the middle of a Petri dish and heated directly with the Bunsen burner. ESCALAB 250Xi was used to execute XPS. Bruker AV 300 was used to execute solid-state NMR.

Electrochemical measurements: The ionic conductivity of the ILE@MOF was measured by electrochemical impedance spectroscopy (CHI660D, China) at various temperatures within the range from -10 to 80 $^{\circ}\text{C}$ and in the frequency range from 10 to 10^5 Hz using an SS/ILE@MOF/SS cell, where SS is stainless steel. The electrochemical anodic stability of the ILE@MOF was assessed by linear sweep voltammetry (LSV) at room temperature, employing a CHI660D workstation at a scan rate of $0.1 \text{ mV}\cdot\text{s}^{-1}$ in conjunction with a Li/ILE@MOF/SS cell. The electrochemical cathodic stability of the ILE@MOF was evaluated by acquiring cyclic voltammograms (CV) at a scan rate of $0.1 \text{ mV}\cdot\text{s}^{-1}$ using the Li/ILE@MOF/SS cell. Li/ILE@MOF/Li symmetric cells were employed during interface stability trials and Li stripping/plating tests. Li/ILE/Li symmetric cells were used for control experiments, with 1 M LiTFSI as the electrolyte and a Celgard separator. Li metal electrodes were collected after stripping/plating tests and were washed with methyl ethyl carbonate in an Ar-filled glove box prior to SEM analysis.

Assembly and performance testing of LMBs: Electrodes were fabricated by mixing 80 wt% electrode material (LiFePO_4 , $\text{LiNi}_{0.33}\text{Mn}_{0.33}\text{Co}_{0.33}\text{O}_2$, $\text{LiNi}_{0.8}\text{Mn}_{0.1}\text{Co}_{0.1}\text{O}_2$ or $\text{Li}_4\text{Ti}_5\text{O}_{12}$), 10 wt% acetylene black and 10 wt% polyvinylidene fluoride (PVDF) in N-methyl-2-pyrrolidone (NMP) to form a viscous slurry that was then cast onto Al foil. The electrodes were heated at 80 $^{\circ}\text{C}$ for 24 h to evaporate the residual solvent then were cut into circular discs with a diameter of 11 mm. The average loading of LiFePO_4 was approximately $4.2 \text{ mg}\cdot\text{cm}^{-2}$, corresponding to $0.7 \text{ mAh}\cdot\text{cm}^{-2}$ based on the theoretical capacity of LiFePO_4 ($170 \text{ mAh}\cdot\text{g}^{-1}$). The average loadings of the $\text{LiNi}_{0.33}\text{Mn}_{0.33}\text{Co}_{0.33}\text{O}_2$, $\text{LiNi}_{0.8}\text{Mn}_{0.1}\text{Co}_{0.1}\text{O}_2$ and $\text{Li}_4\text{Ti}_5\text{O}_{12}$ were 3.7, approximately 4.0 and $3.9 \text{ mg}\cdot\text{cm}^{-2}$. LMBs were prepared in an Ar-filled glove box by placing the electrodes, ILE@MOF and Li metal in a CR2032 button cell to form a cell without any separator. The charge/discharge cycling of LMBs was performed using a Land instrument. The Li/ LiFePO_4 cells were discharged between 2.7 and 4.2 V at 0.1 C ($1.0 \text{ C}=170 \text{ mA}\cdot\text{g}^{-1}$) at 60 $^{\circ}\text{C}$. The Li/ $\text{LiNi}_{0.33}\text{Mn}_{0.33}\text{Co}_{0.33}\text{O}_2$ cells were charged/discharged between 2.8 and 4.2 V at 2.0 C ($1.0 \text{ C}=140 \text{ mA}\cdot\text{g}^{-1}$) at 60, 90, 120 and 150 $^{\circ}\text{C}$. The Li/ $\text{LiNi}_{0.8}\text{Mn}_{0.1}\text{Co}_{0.1}\text{O}_2$ cells were charged/discharged between 2.7 and 4.3 V at 2.0 C ($1.0 \text{ C}=150 \text{ mA}\cdot\text{g}^{-1}$) at 150 $^{\circ}\text{C}$. The Li/ $\text{Li}_4\text{Ti}_5\text{O}_{12}$ cells were charged/discharged between 1.0 and 2.5 V at 1.0 C ($1.0 \text{ C}=170 \text{ mA}\cdot\text{g}^{-1}$) at 150 $^{\circ}\text{C}$. The Li metal electrode, ILE@MOF electrolyte and cathode electrode were washed with methyl ethyl carbonate and stored in an Ar-filled glove box for SEM analysis. Electrochemical impedance spectroscopy was performed with a CHI660D apparatus at various temperatures. Electrochemical stability data were obtained from CV results acquired with a CHI660D workstation at a scan rate of $0.1 \text{ mV}\cdot\text{s}^{-1}$.

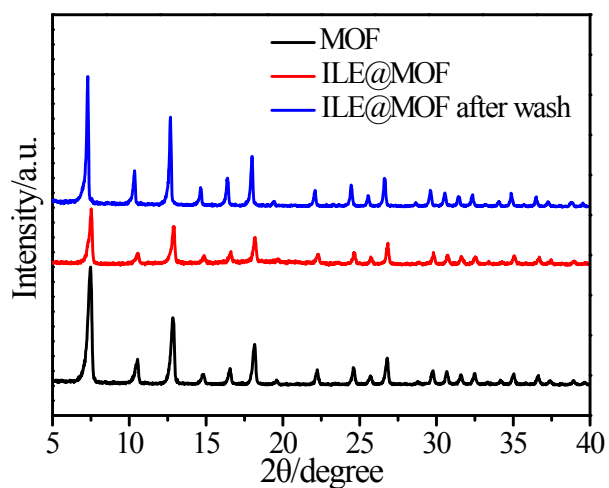


Figure S1. XRD pattern of MOF, ILE@MOF electrolyte, and ILE@MOF after wash with acetonitrile to removal of the ILE.

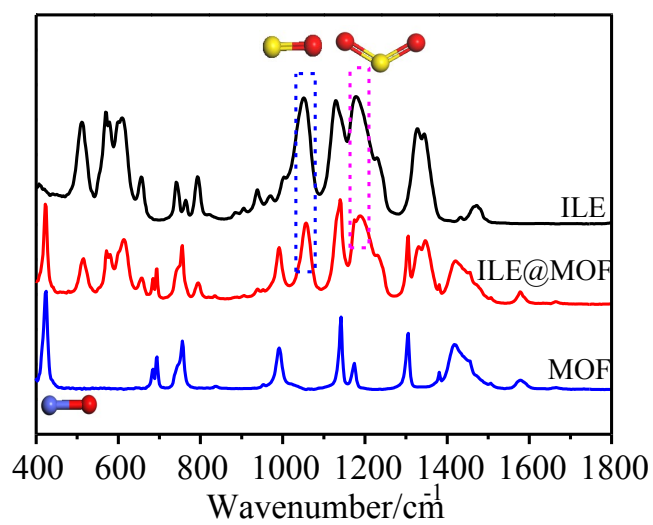


Figure S2. FTIR spectra of MOF, ILE@MOF and ILE.

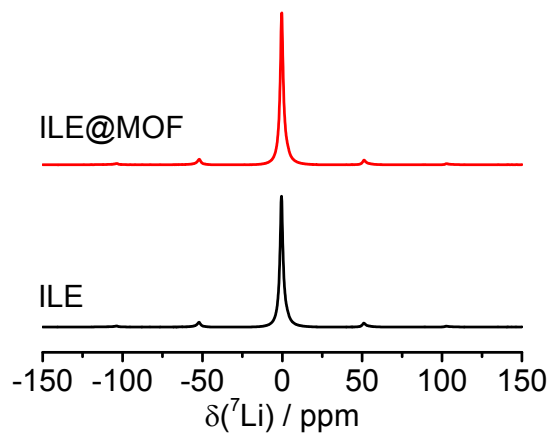


Figure S3 ^7Li NMR spectra for ILE and ILE@MOF.

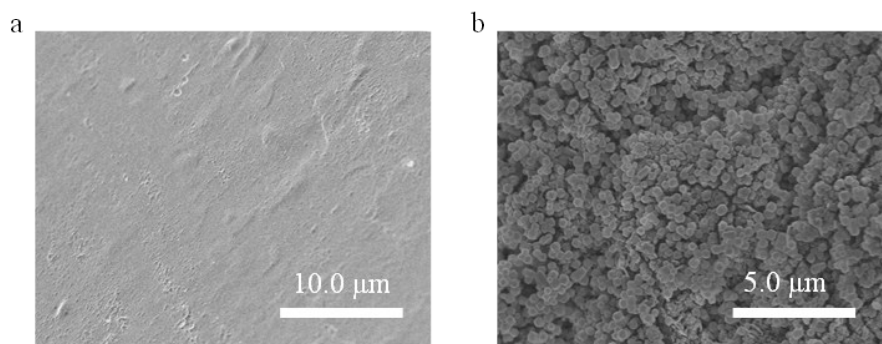


Figure S4 a) SEM images of a fresh Li metal. b) SEM images of Li metal surface in the Li/ILE@MOF/Li cell before cycling.

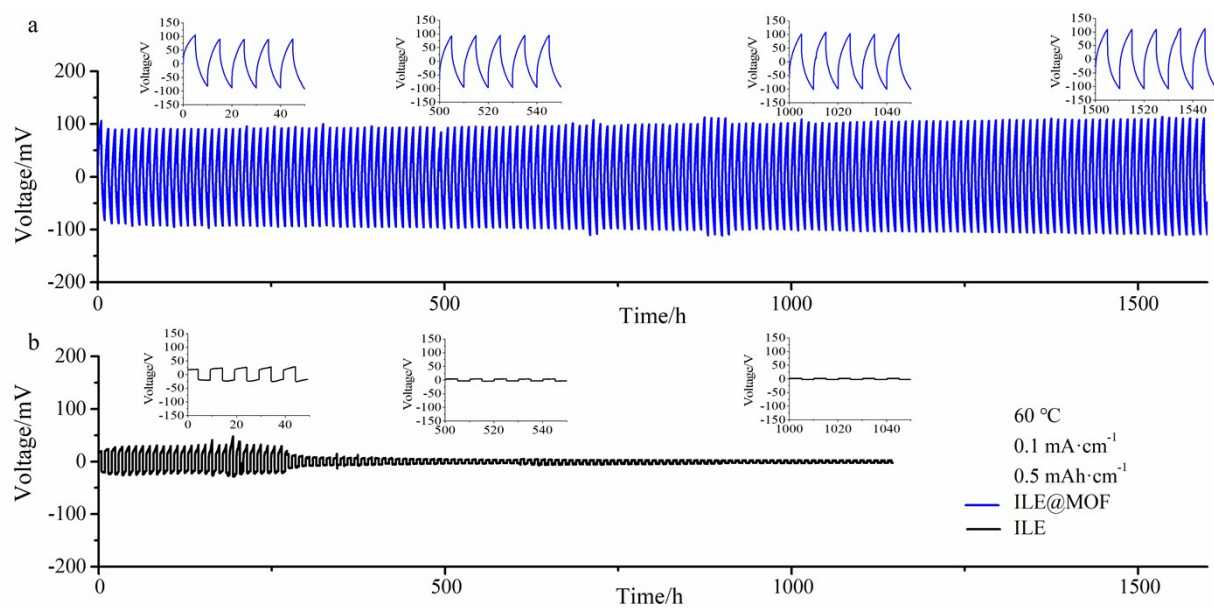


Figure S5 a) Voltage profiles for Li/ILE@MOF/Li cell cycling at a current density of $0.1 \text{ mA} \cdot \text{cm}^{-2}$ at $60 \text{ }^\circ\text{C}$. Each cycle is set to be 10 h. b) Voltage profiles for Li/ILE /Li cell cycling at a current density of $0.1 \text{ mA} \cdot \text{cm}^{-2}$ at $60 \text{ }^\circ\text{C}$. Each cycle is set to be 10 h.

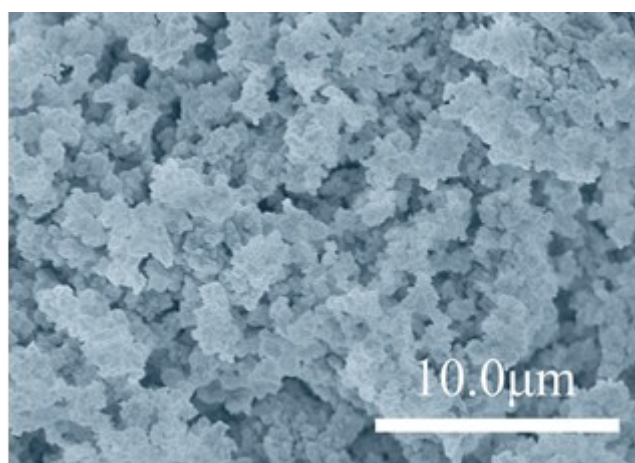


Figure S6 f) SEM morphology for Li anode in Li/ILE /Li cell after 1000 h cycling at $0.1 \text{ mA} \cdot \text{cm}^{-2}$ at $60 \text{ }^\circ\text{C}$.

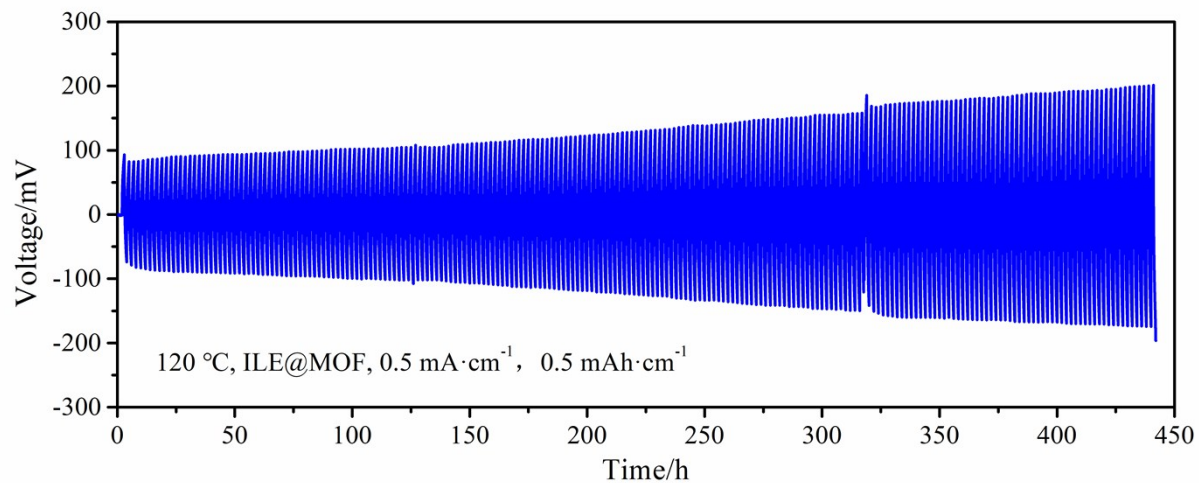


Figure S7 Voltage profiles for Li/ILE@MOF/Li cell cycling at a current density of $0.5 \text{ mA}\cdot\text{cm}^{-2}$ at $120 \text{ }^\circ\text{C}$. Each cycle is set to be 2 h.

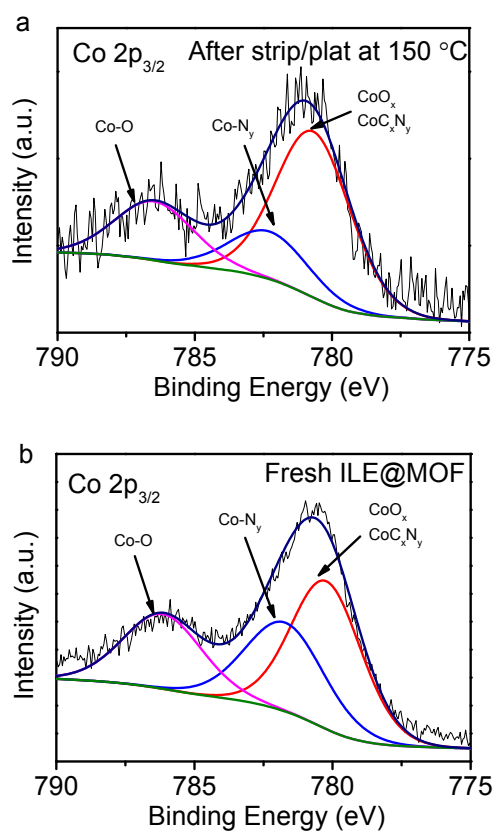


Figure S8 a) Co 2P XPS spectra for the thin particles layer of Li metal after 100 h stripping/plating at 150 °C. b) Co 2P XPS spectra of fresh ILE@MOF electrolyte.

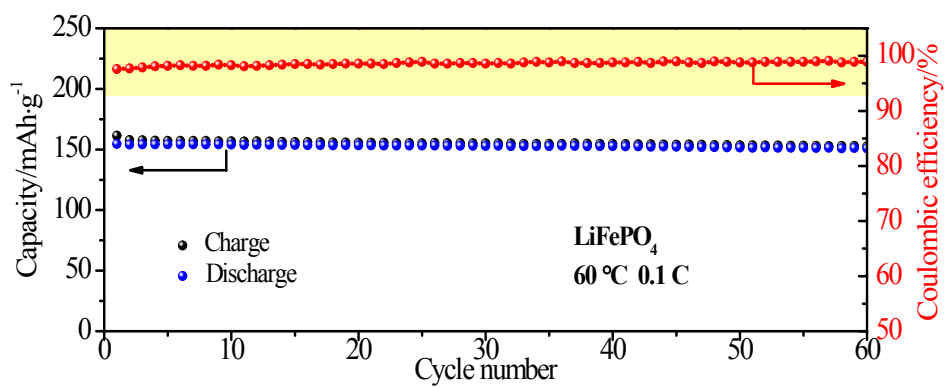


Figure S9 Cycle performance of the Li/LiFePO₄ cells using the ILE@MOF electrolyte at 60 °C.

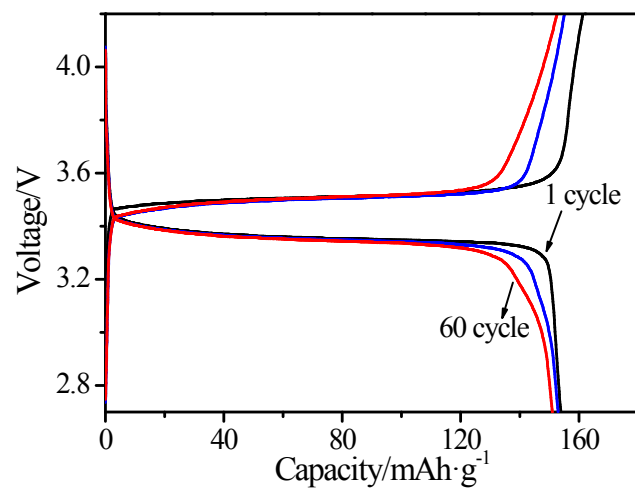


Figure S10 Galvanostatic charge/discharge plots of Li/LiFePO₄ cell using the ILE@MOF electrolyte.

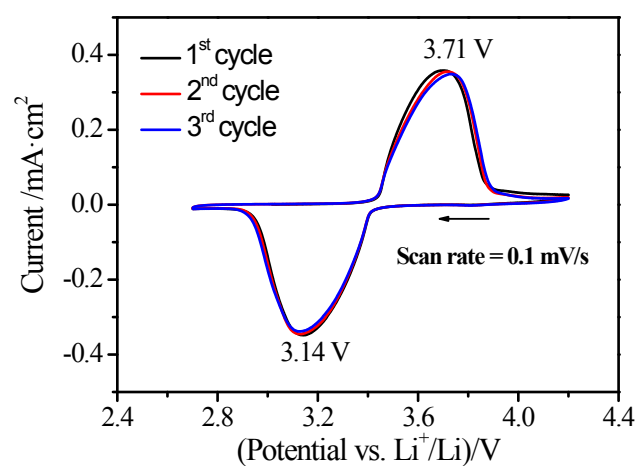


Figure S11 Cyclic voltammograms of the Li/LiFePO₄ cell using ILE@MOF electrolyte.

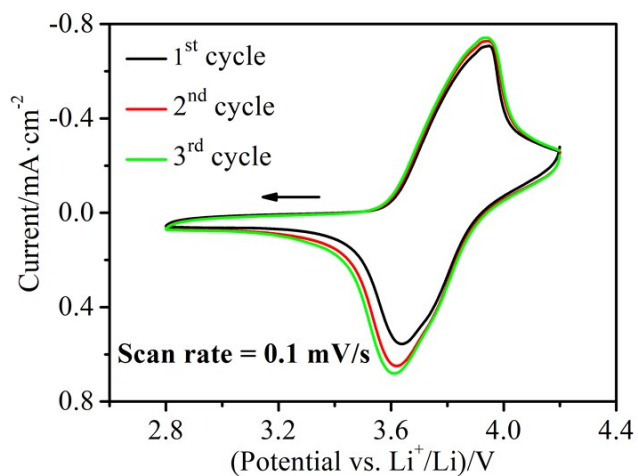


Figure S12 Cyclic voltammograms of the $\text{Li}/\text{LiNi}_{0.33}\text{Mn}_{0.33}\text{Co}_{0.33}\text{O}_2$ cell using ILE@MOF electrolyte.

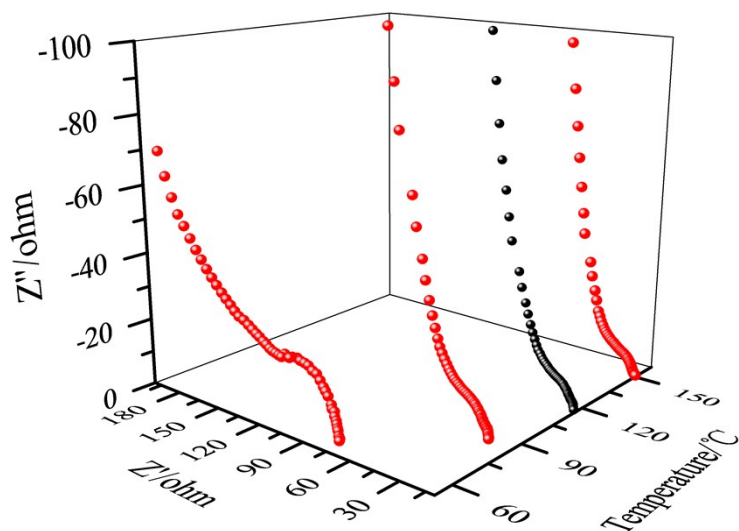


Figure S13 Electrochemical impedance spectra (EIS) of $\text{Li}/\text{LiNi}_{0.33}\text{Mn}_{0.33}\text{Co}_{0.33}\text{O}_2$ cell using ILE@MOF electrolyte at 60, 90, 120, and 150 °C.

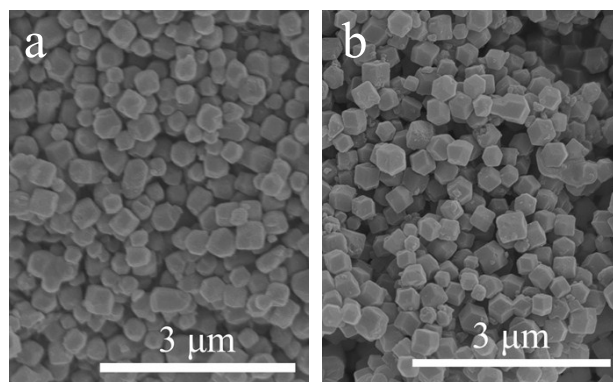


Figure S14 SEM images of $\text{LiNi}_{0.33}\text{Mn}_{0.33}\text{Co}_{0.33}\text{O}_2$ electrode surface after initial discharged at a) 90 °C and b) 120 °C.

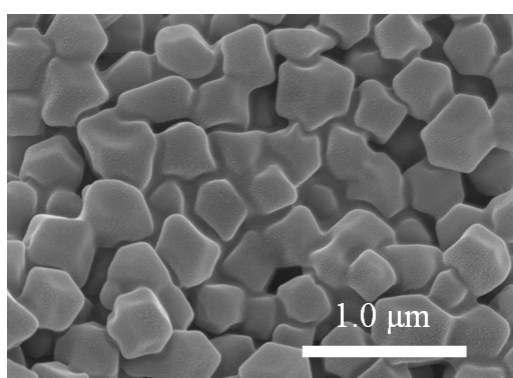


Figure S15 SEM images of dense MOF on the surface of cycled $\text{LiNi}_{0.33}\text{Mn}_{0.33}\text{Co}_{0.33}\text{O}_2$ electrode.

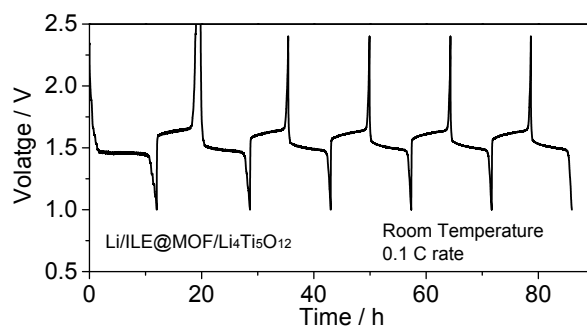


Figure S16 The voltage profiles of $\text{Li}/\text{ILE@MOF}/\text{Li}_4\text{Ti}_5\text{O}_{12}$ cell at rate of 0.1 C and at room temperature.

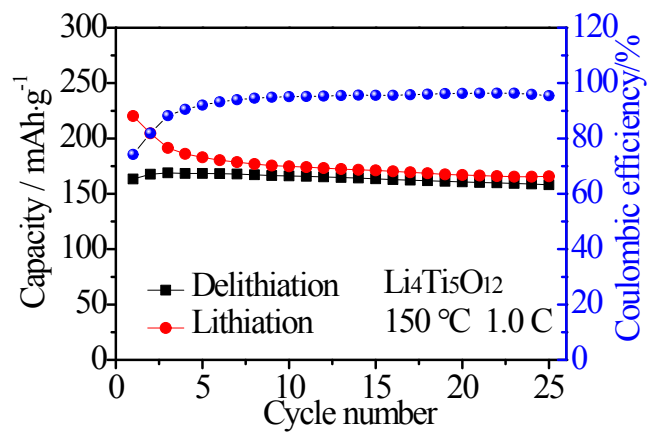


Figure S17 Cycling performances of Li/Li₄Ti₅O₁₂ cell using the ILE@MOF electrolyte at a current density of 1.0 C at 150 °C.

Table S1 Summarized the BET information.

| Materials | MOF | ILE@MOF- 0.2M LiTFSI | ILE@MOF- 0.6M LiTFSI | ILE@MOF- 1.0M LiTFSI |
|--------------------------------------|-----------|-------------------------|-------------------------|-------------------------|
| Specific surface (m ² /g) | 1352.1974 | 2.6145 | 2.1754 | 0.0087 |

The BET result revealed that the specific surface of MOF is 1352.1974 m²/g. and the specific surface of ILE@MOF decreases from 1791.88 m²/g to 5.26 m²/g by introducing of ILE.

Table S2 Summarized the fundamental security information of different electrolytes

| Electrolyte | Thermal stability | Electrode | Test temperature | Cycle performance (mAh·g ⁻¹) | Ref. |
|---|-------------------|--|----------------------------|---|----------|
| ILE@MOF | 325 °C | LiNi _{0.33} Mn _{0.33} Co _{0.33} O ₂ LiNi _{0.8} Mn _{0.1} Co _{0.1} O ₂ Li ₄ Ti ₅ O ₁₂ | 150 °C 150 °C 150 °C | 143.5 at 2.0 C 137.3 at 2.0 C ~165 at 1.0 C | Our work |
| Liquid | | | | | |
| 1M LiPF ₆ -EC/EMC/DMC | 40 °C | LiNi _{0.33} Mn _{0.33} Co _{0.33} O ₂ | 25 °C | 190 at 0.1 C | [2] |
| LiTFSI/[EMIm][FSI] | 220 °C | LiNi _{0.33} Mn _{0.33} Co _{0.33} O ₂ | RT | 163 at 1.0 C | [3] |
| 1M LiPF ₆ -EC/DMC/EMC+PP13TFSI | 100 °C | LiNi _{0.33} Mn _{0.33} Co _{0.33} O ₂ | RT | 230 at 0.1 C | [4] |
| LiTFSI-EC/DMC+[Py14][TFSI] | 100 °C | LiFePO ₄ | RT | 150 at 0.1 C | [5] |
| Ionogel | | | | | |
| h-BN/[PP13][TFSI]/LiTFSI | - | Li ₄ Ti ₅ O ₁₂ | 150 °C | ~145 at 0.5 C | [6] |
| Clay/[PP13][TFSI]/LiTFSI | 370 °C | Li ₄ Ti ₅ O ₁₂ | 120 °C | ~60 at 1/3 C | [7] |
| SiO ₂ /[BMI][TFSI]/LiTFSI | 390 °C | LiNi _{0.33} Mn _{0.33} Co _{0.33} O ₂ | 30 °C | ~149 at 0.1 C | [8] |
| TiO ₂ /[Py13][TFSI]/LiTFSI | 375 °C | LiNi _{0.33} Mn _{0.33} Co _{0.33} O ₂ | RT | 120 at 0.1 C | [9] |
| SiO ₂ -PP-TFSI/PC/1M LiTFSI | 250 °C | Li ₄ Ti ₅ O ₁₂ | RT | 130 at 1.0 C | [10] |
| Gel polymer | | | | | |
| PVdF/P(VC-VAc)-1M LiPF ₆ -EC/EMC/DMC | 240 °C | LiNi _{0.5} Mn _{1.5} O ₄ | RT | 127 at 0.5 C | [11] |
| PEO-LiTFSI-EMIMTFSI | 310 °C | LiMn ₂ O ₄ | RT | 120 at 0.1 C | [12] |
| LiTFSI-[PP14][TFSI]-P(VdF-HFP) | 150 °C | LiFePO ₄ | 60 °C | 131 at 1.0 C | [13] |

RT: Room Temperature

References

- [1] Z. Wang, J. Liu, C. Li, P. Zhang and H. Zhuo, *International Journal of Electrochemical Science* 2016, **11**, 6149-6163.
- [2] K. Matsumoto, S. Sogabe and T. Endo, *Journal of Polymer Science Part A: Polymer Chemistry* 2012, **50**, 1317-1324.
- [3] Y. Matsui, S. Kawaguchi, T. Sugimoto, M. Kikuta, T. Higashizaki, K. Michiyuki, M. Yamagata and M. Ishikawa, *Electrochemistry* 2012, **80**, 808-811.
- [4] H. Li, J. Pang, Y. Yin, W. Zhuang, H. Wang, C. Zhai and S. Lu, *RSC Advances* 2013, **3**, 13907-13914.
- [5] M. Agostini, L. G. Rizzi, G. Cesareo, V. Russo and J. Hassoun, *Advanced Materials Interfaces* 2015, **2**, 1500085.
- [6] M. T. F. Rodrigues, K. Kalaga, H. Gullapalli, G. Babu, A. L. M. Reddy and P. M. Ajayan, *Advanced Energy Materials* 2016, **6**, 201600218.
- [7] K. Kalaga, M.-T. F. Rodrigues, H. Gullapalli, G. Babu, L. M. R. Arava and P. M. Ajayan, *ACS Applied Materials & Interfaces* 2015, **7**, 25777-26783.
- [8] G. Tan, F. Wu, C. Zhan, J. Wang, D. Mu, J. Lu and K. Amine, *Nano Letters* 2016, **16**, 1960-1968.
- [9] F. Wu, N. Chen, R. Chen, Q. Zhu, G. Tan and L. Li, *Advanced Science* 2016, **3**, 1500306.
- [10] Y. Lu, K. Korf, Y. Kambe, Z. Tu and L. A. Archer, *Angewandte Chemie* 2014, **53**, 488-492.
- [11] M. Zhao, X. Zuo, X. Ma, X. Xiao, J. Liu and J. Nan, *Journal of Membrane Science* 2017, **532**, 30-37.
- [12] L. Balo, Shalu, H. Gupta, V. Kumar Singh and R. Kumar Singh, *Electrochimica Acta* 2017, **230**, 123-131.
- [13] L. Liu, P. Yang, L. Li, Y. Cui and M. An, *Electrochimica Acta* 2012, **85**, 49-56.